Les Cahiers du GERAD ISSN: 0711–2440

Blackbox optimization for origami-inspired bistable structures

Supplementary material

L. Boisneault, C. Audet, D. Melancon

G–2024–51

Août 2024

La publication de ces rapports de recherche est rendue possible grâce au soutien de HEC Montréal, Polytechnique Montréal, Université McGill, Université du Québec à Montréal, ainsi que du Fonds de recherche du Québec – Nature et technologies.

Dépôt légal – Bibliothèque et Archives nationales du Québec, 2024
– Bibliothèque et Archives Canada, 2024

The publication of these research reports is made possible thanks to the support of HEC Montréal, Polytechnique Montréal, McGill University, Université du Québec à Montréal, as well as the Fonds de recherche du Québec – Nature et technologies.

Legal deposit – Bibliothèque et Archives nationales du Québec, 2024
– Library and Archives Canada, 2024

GERAD HEC Montréal
3000, chemin de la Côte-Sainte-Catherine
Montréal (Québec) Canada H3T 2A7

Tél. : 514 340-6053
Téléc. : 514 340-5665
info@gerad.ca
www.gerad.ca

Blackbox optimization for origami-inspired bistable structures

Supplementary material

Luca Boisneault [a, c]
Charles Audet [b, d]
David Melancon [a, c]

[a] *Laboratory for Multiscale Mechanics (LM2), Department of Mechanical Engineering, Polytechnique Montréal, Montréal (Qc), Canada, H3T 1J4*

[b] *Department of Mathematical and Industrial Engineering, Polytechnique Montréal, Montréal (Qc), Canada, H3T 1J4*

[c] *Research Center for High Performance Polymer and Composite Systems (CREPEC), Department of Mechanical Engineering, McGill University, Montréal (Qc), Canada, H3A 0C3*

[d] *GERAD, Montréal (Qc), Canada, H3T 1J4*

luca.boisneault@polymtl.ca
david.melancon@polymtl.ca

Août 2024
Les Cahiers du GERAD
G–2024–51

Abstract : Bistable mechanical systems exhibit two stable configurations where the elastic energy is locally minimized. To realize such systems, origami techniques have been proposed as a versatile platform to design deployable structures with both compact and functional stable states. Conceptually, a bistable origami motif is composed of two-dimensional surfaces connected by one-dimensional fold lines. This leads to stable configurations exhibiting zero-energy local minima. Physically, origami-inspired structures are three-dimensional, comprising facets and hinges fabricated in a distinct stable state where residual stresses are minimized. This leads to the dominance of one stable state over the other. To improve mechanical performance, one can solve the constrained optimization problem of maximizing the bistability of origami structures, defined as the amount of elastic energy required to switch between stable states, while ensuring materials used for the facets and hinges remain within their elastic regime. In this study, the Mesh Adaptive Direct Search (Mads) algorithm, a blackbox optimization technique, is used to solve the constrained optimization problem. The bistable waterbomb-base origami motif is selected as a case-study to present the methodology. The elastic energy of this origami pattern under deployment is calculated via Finite Element simulations which serve as the blackbox in the Mads optimization loop. To validate the results, optimized waterbomb-base geometries are built via Fused Filament Fabrication and their response under loading is characterized experimentally on a Uniaxial Test Machine. Ultimately, our method offers a general framework for optimizing bistability in mechanical systems, presenting opportunities for advancement across various engineering applications.

Keywords : Origami, multistability, blackbox optimization, Finite Element method

Acknowledgements: **Funding:** This work was funded by Audet's NSERC Canada Discovery Grant 2020–04448 and by Melancon's research start-up grant from Polytechnique Montréal. **Author contributions:** L.B., C.A., and D.M. proposed and developed the research idea. L.B. performed the FEM simulations, fabricated the physical prototypes, and developed and ran the blackbox optimization. L.B., C.A. and D.M. wrote the paper. C.A. and D.M. supervised the research. **Competing interests:** The authors declare no conflict of interest. **Data and materials availability:** The data that support the findings of this study are available on request from the corresponding author. The optimization code described schematically in Fig. **??** is available on Github at `https://github.com/lm2-poly/OriMads`.

1 Fabrication of the waterbomb pattern

Each sample of the waterbomb is fabricated using Fused Filament Fabrication (FFF). The steps to obtained the physical prototypes presented in the main article are presented in Fig. 1 and listed below.

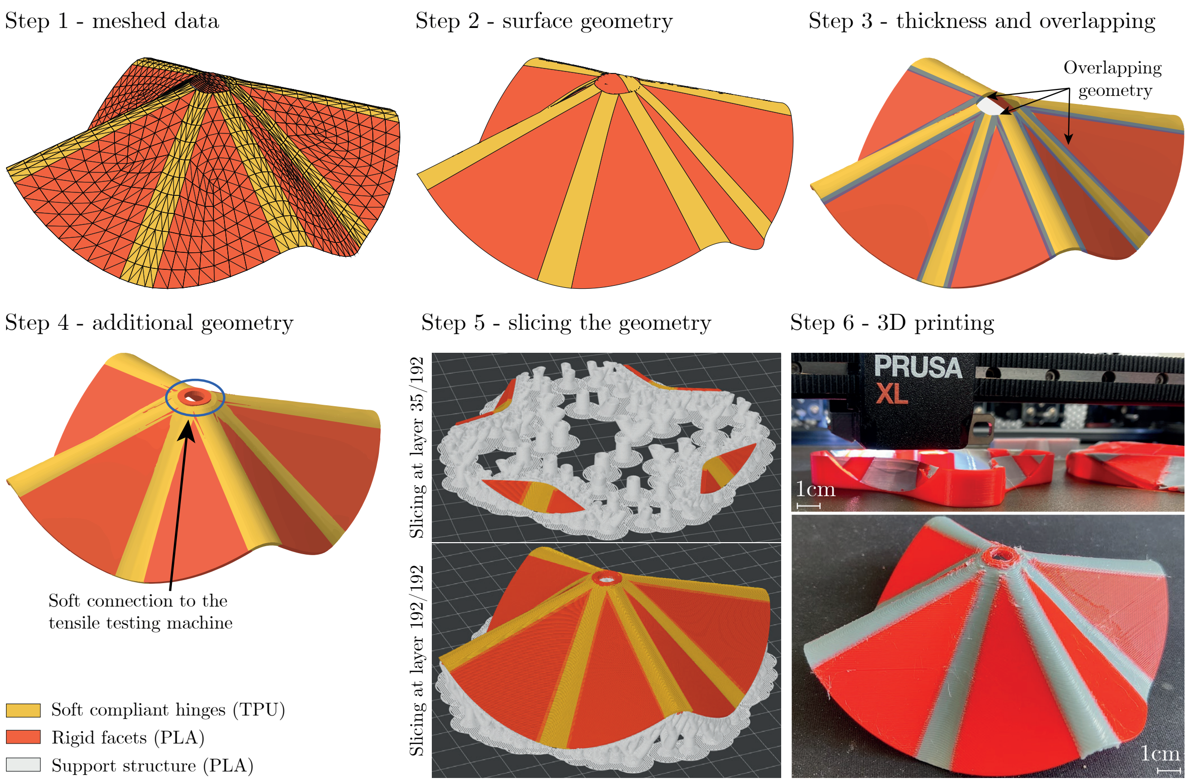

Figure 1: Fabrication of the waterbomb origami pattern from the FEM data to FFF multimaterial 3D printing.

Step 1: Retrieve the meshed geometry of the initial shape of the **actuation** phase described in Fig. 2 of the main article.

Step 2: Convert the mesh data to a smooth surface using the *Geometry Edit* feature of Abaqus. Export the edited model as a `.step` file.

Step 3: Import the `.step` file into a CAD software (Catia). Assign surface thickness and an overlapping geometry of 1 mm width each intersection of the facets and the compliant crease to ensure the interlacing of material when 3D printing. This additional geometry ensures proper bonding between both the rigid and the soft regions.

Step 4: Fill the inner hole with soft material as well as a stiffer platform for assembly with the tensile testing machine.

Step 5: Slice the geometry using the software PrusaSlicer. The supports are generated automatically.

Step 6: Print samples on a PrusaXL using two of the five printing heads available. Note that the three additional heads could be used to implement more materials in the origami geometry. PLA from the supplier Raise3D and TPU from Eryone were used to print the facets and the creases, respectively.

2 Mechanical testing of the waterbomb pattern

Inspired by the methodology employed by Hanna et al. Hanna et al. (2014), the waterbomb origami pattern is tested under punctual loading on a uniaxial tensile testing machine. Because of its bistable behavior, the force will eventually switch direction, i.e., the sample will not lay on the test bench anymore and no value of reaction force will be measured.

For this reason, one needs to measure both responses independently: from state 1 to state 2 (direction a), and separately from state 2 to state 1 (direction b). In direction a, the mountain hinges of the waterbomb rest on triangular rails (Fig. 2a). In a second phase, the waterbomb is flipped, and the same mountain folds now rest on flat surfaces as shown in Fig. 2b. The sample is connected to a 100N load cell via a standard M6 screw (see Fig. 2c). Both sides are tested and, as expected, direction b displays a reaction force response three times lower than direction a in the first graph of Fig. 2d. This is due to the residual stress: less energy is required to switch back to the first state. The complete energy curve is constructed as an assembly of the two energy responses. Direction b is placed at the end of direction a as displayed in the second curve of Fig. 2d. The energy curve is then extracted as the work of the force across the displacement of the central node.

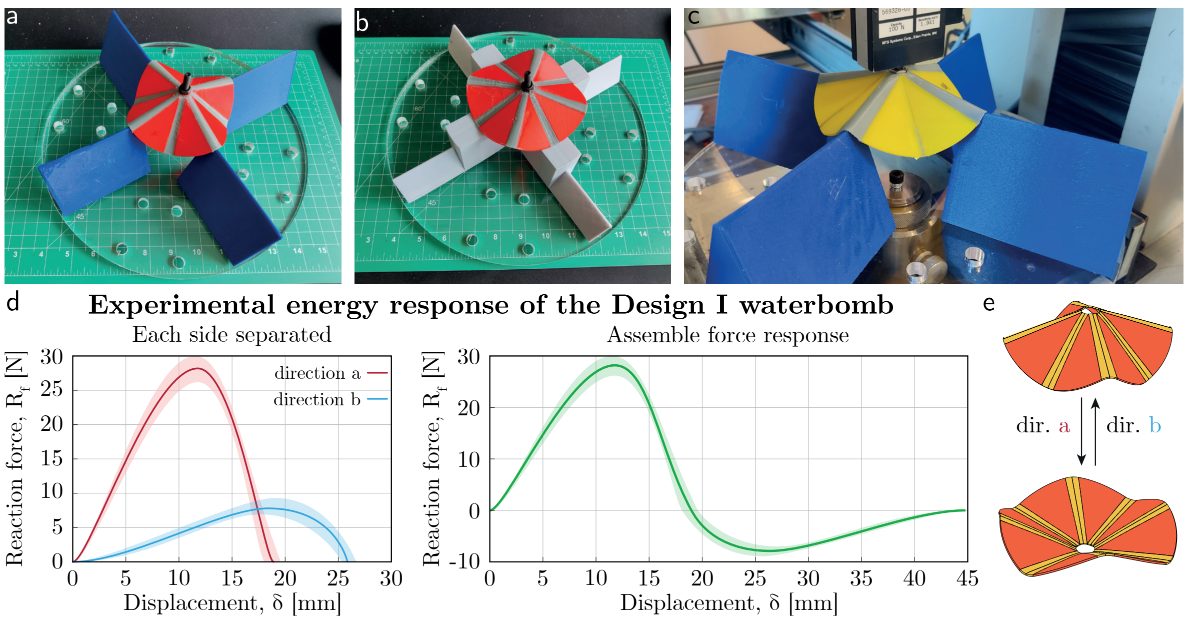

Figure 2: Experimental testing of the waterbomb pattern: a. Testing setup in direction a, from the first to the second stable state, with the attachment bolt on. b. Experimental setup of the waterbomb to switch from the second to the first state (direction b). c. Waterbomb fitted in the tensile testing machine. d. Representative force-displacement curves recorded during the loading in the two directions and total assembled force-displacement of the waterbomb structure. Shaded areas represent the standard deviation from multiple samples tested. e. Schematics of the waterbomb in the two stable configurations along with the directions of switching.

3 Additional optimization results

The optimization process developed in the article is applied to a bistable origami star to demonstrate the efficiency of the method on other origami structures. This basic origami shape has been used as a building block to create meter scale functional structures such as arches and shelters Melancon et al. (2021). Compared to the waterbomb pattern with two non-flat stable states, the bistable origami star exhibits both a flat and a deployed stable configuration (see Fig. 3a). Its energy response under deployment can be calculated using FEM (Fig. 1b), by modeling only $1/(4n)$ of the structure, where $n = 4$, the number of branches. This can be done as the star pattern is based on three planar symmetries: one vertical (xy-plane) and two cyclic symmetries ($z\theta$-plane) on both sides. A vertical displacement is imposed on the rigid facet at the node that is closest to the center of the star. The boundary conditions are displayed in Fig. 3c.

This origami structure can be parameterized both using global design variables to define the general pattern and local variables to modify the crease shapes, as shown in Fig. 3d. The global variables are R_i, the length of the shortest side of the star; R_e, the length of the longest side of the star; and ω, the ratio of thicknesses between the soft hinges and the rigid facets. For the compliant crease geometry, four additional variables are implemented: r, the radius of the central hole; α, the normalized angle defining the position of the node where the displacement is imposed; h, the height of the vertical crease; and l_1 and l_2, which characterize the width at the tip of the creases of the longest and shortest sides, respectively.

An optimization using Mads is conducted with the objective function $\phi = f(r, \alpha, l_1, l_2, R_i, R_e)$. The number of design variables considered in the optimization process can be adapted to the needs of the application for which the bistable star will be used. Optimization is launched from the point $x^0 = (13.1, 0.5, 5.0, 5.0, 58.9, 85.9)$, defining a shape where the width of the creases is uniform across the structure. This initial configuration provides a bistable performance $\phi^0 = 9.0\%$. The lower and upper boundary conditions for the optimization, respectively l_b and u_b, are defined by:

- $l_b = (5.0, 0.0, 0.0, 0.0, 50.0, 50.0)$,
- $u_b = (35.0, 1.0, 10.0, 10.0, 150.0, 150.0)$.

After 350 evaluations, the process outputted an improved shape defined by $x^* = (26.1, 0.8, 4.3, 3.3, 85.5, 102.2)$ and an improved bistable performance $\phi^* = 72.6\%$. One can note that none of the design variables ended up reaching the boundary conditions in the improved configuration. The convergence graph of this optimization is displayed in Fig. 3e. The plot exhibits a large number of failed evaluations, as is the case for the optimization of the waterbomb. When the optimization is stopped, i.e., after 350 evaluations, the plot exhibits a great increase within the first 50 evaluations and keeps growing until the stopping criterion is reached.

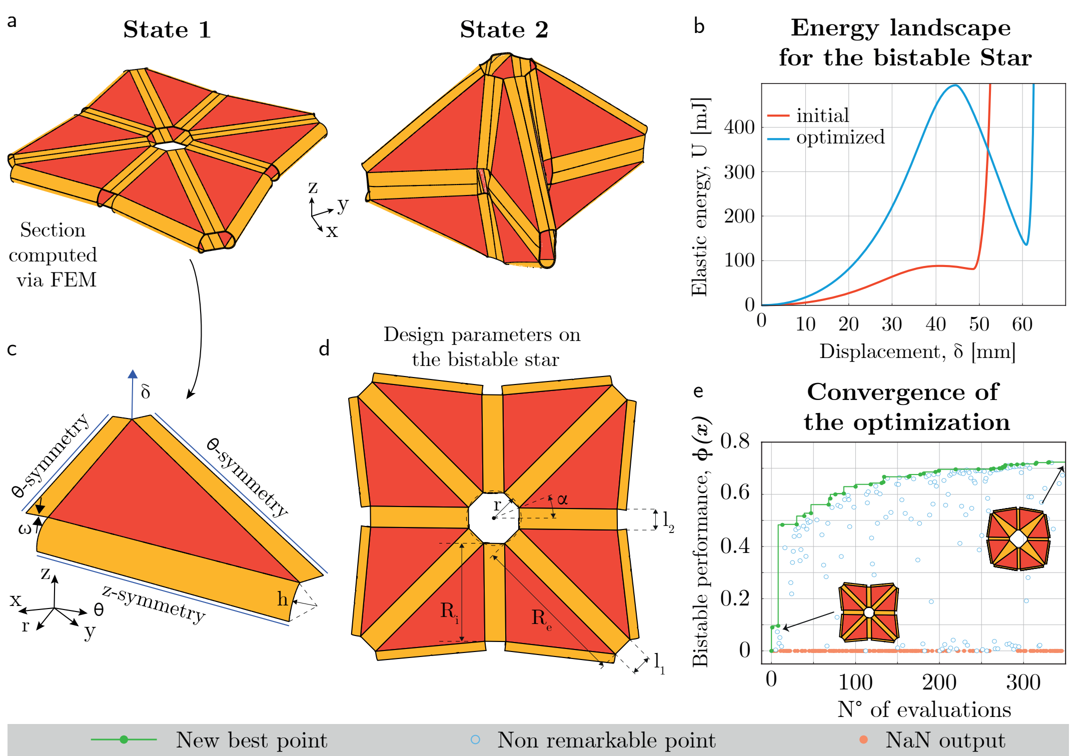

Figure 3: Numerical model of the bistable star origami: a. Bistable star in both the compact (state 1) and the deployed (state 2) configurations. b. An energy-displacement curve exhibiting both the initial and the final shapes of the optimization. c. Finite Element model and the associated boundary conditions. d. The bistable star parameterized with all the available design variables. e. Convergence of the objective function (bistable performance) of the optimization.

References

Hanna, B. H., Lund, J. M., Lang, R. J., Magleby, S. P., and Howell, L. L. (2014). Waterbomb base: a symmetric single-vertex bistable origami mechanism. Smart Materials and Structures, 23(9):094009.

Melancon, D., Gorissen, B., García-Mora, C. J., Hoberman, C., and Bertoldi, K. (2021). Multistable inflatable origami structures at the metre scale. Nature, 592(7855):545–550.